

# Reducing Spurious Correlation for Federated Domain Generalization

Shuran Ma  
shrma@stu.xidian.edu.cn  
Xidian University  
Xi'an, Shaanxi, China

Weiyong Xie  
wyxie@xidian.edu.cn  
Xidian University  
Xi'an, Shaanxi, China

Daixun Li  
ldx@stu.xidian.edu.cn  
Xidian University  
Xi'an, Shaanxi, China

Haowei Li  
23011210779@stu.xidian.edu.cn  
Xidian University  
Xi'an, Shaanxi, China

Yunsong Li  
ysli@mail.xidian.edu.cn  
Xidian University  
Xi'an, Shaanxi, China

## ABSTRACT

The rapid development of multimedia has provided a large amount of data with different distributions for visual tasks, forming different domains. Federated Learning (FL) can efficiently use this diverse data distributed on different client media in a decentralized manner through model sharing. However, in open-world scenarios, there is a challenge: global models may struggle to predict well on entirely new domain data captured by certain media, which were not encountered during training. Existing methods still rely on strong statistical correlations between samples and labels to address this issue, which can be misleading, as some features may establish spurious short-cut correlations with the predictions. To comprehensively address this challenge, we introduce *FedCD* (Cross-Domain Invariant Federated Learning), an overall optimization framework at both the local and global levels. We introduce the Spurious Correlation Intervener (SCI), which employs invariance theory to locally generate interveners for features in a self-supervised manner to reduce the model's susceptibility to spurious correlated features. Our approach requires no sharing of data or features, only the gradients related to the model. Additionally, we develop the simple yet effective Risk Extrapolation Aggregation strategy (REA), determining aggregation coefficients through mathematical optimization to facilitate global causal invariant predictions. Extensive experiments and ablation studies highlight the effectiveness of our approach. In both classification and object detection generalization tasks, our method outperforms the baselines by an average of at least 1.45% in *Acc*, 4.8% and 1.27% in *mAP*<sub>50</sub>. The code is released at:xxx.

## CCS CONCEPTS

• **Computing methodologies** → **Computer vision**; *Distributed algorithms*.

## KEYWORDS

Federated Learning, Domain Generalization, Spurious Correlation

## 1 INTRODUCTION

The swift evolution of multimedia technology has provided us with a rich and diverse data resource, greatly advancing the development of visual tasks. The diversity of multimedia data is reflected not only in the wide range of artistic forms, such as visual arts, photography, and animation but also in the different environments considering the autonomous driving scenarios, such as scenes and weather conditions. These diverse data samples are valuable materials that have significantly enhanced the ability of neural networks to understand and process visual information. Faced with strict requirements for privacy protection, traditional centralized learning methods are limited by the risk of privacy leakage, making it difficult to utilize multimedia data. Federated Learning (FL), as an emerging machine learning framework, provides an effective solution. FL allows multiple devices or medias to train models locally and improve the global model collaboratively by sharing model updates or gradients instead of raw data. The rapid rise of new media continuously introduces new domain data, which poses requirements for domain generalization, referring to the ability of a model to maintain good performance when faced with new domain data distributions that differ from the training set. Although federated learning facilitates the joint training of different media data, it is not sufficient to address this issue, as it still relies on simple collaborative training of client data and may struggle to predict on unseen domains.

There have been some early works aiming to address the aforementioned issue. Representation learning was utilized in [27, 33, 48] to tackle this challenge by considering various aspects such as conditional mutual information and the distribution of features across different clients. Liu *et al.* employed meta-learning which is considered programming-unfriendly in [22]. Additionally, this work shared amplitude spectrum which is data-related, potentially contradicting the principles of federated learning. Qu *et al.*[28] improved domain generalization by providing a flatter, more generalized loss function. However, these methods still utilized all features unbiasedly, which means they used all features without intervention and allowed the neural network to establish connections between any features and predictions based solely on statistical correlations, without considering that some of these correlations might be spurious shortcuts. However, we think they are insufficient because only

Permission to make digital or hard copies of all or part of this work for personal or professional use, is granted by ACM for individuals and small organizations, not for profit or commercial advantage and that copies bear this notice and the full citation on the first page. Copyrights for components of this work owned by others than the author(s) must be honored. Abstracting with credit is permitted. To copy otherwise, or to publish, to post on servers or to redistribute to lists, requires prior specific permission and/or a fee. Request permissions from permissions@acm.org.

ACM MM, 2024, Melbourne, Australia  
© 2024 Copyright held by the owner/author(s). Publication rights licensed to ACM.  
ACM ISBN 978-x-xxxx-xxxx-x/YY/MM  
<https://doi.org/10.1145/nnnnnnn.nnnnnn>

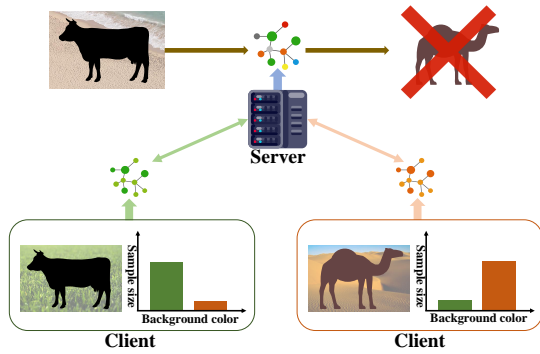


**Figure 1: The "Cow-On-The-Beach" problem in FL. Local models on the client side strongly correlate cows with green grassland and camels with beige deserts within the samples. Thus, replacing the background of the cow with a beige beach may lead to incorrect prediction on global model.**

a subset of the target's features in the sample ultimately leads to predictions, excluding features related to the scene, style or other aspects of the target, such as the color of the car. Therefore, we should not consider all of them when making predictions, or at least not unbiasedly, which can provide a more thorough understanding and stable performance.

To achieve a more comprehensive improvement, we will delve deeper into the spurious correlations between data features and predictions. As shown in Figure 1, inspired by the "cow-on-the-beach" example presented in [2], neural networks rely on simple statistical relationships, e.g., cow and green grass to make predictions, which establishes a strong correlation between a green background and a cow, leading to wrong predictions when the background changes to a beige beach. We believe that the model's capture of spurious "short-cut" features hinders generalization. Inspired by some non-causal and invariance theories [13, 41] that reduce spurious correlations, we locally design a **Spurious Correlation Intervener (SCI)** to mitigate the impact of spurious features on model training. Additionally, leveraging causal invariance theory [2, 14], we propose the **Risk Extrapolation Aggregation strategy (REA)** from a causal inference perspective.

Within the *SCI*, we reference the principle of invariance to design a self-supervised feature intervener, aiming to reduce the impact of spurious correlated features. Moreover, the training of *SCI* only requires the sharing of model-related gradients, without violating the principles of federated learning, and is even more lightweight than sharing data-related information. In light of insights from [2, 14], which affirm the relationship between training risk and the causal invariance mechanism of domain generalization, we propose the simple yet effective *REA* strategy during aggregation. This strategy transforms the fixed aggregation coefficients into a set of solutions for the risk extrapolation optimization problem, further enhancing global invariant causal predictions.

Our main contributions are highlighted as follows:

- We aim to address the federated domain generalization problem by considering spurious correlations. We locally and

self-supervisedly train feature interveners for each client, while also considering the strong prior dependence on causal invariant components of images, and the constraints thereby imposed. Additionally, we provide a detailed theoretical derivation of the training objective.

- We introduce *REA*, a novel aggregation strategy that recalculates aggregation coefficients through a simple yet effective risk extrapolation optimization problem which does not require the introduction of new network structures for solving, making it efficient and easy to implement.
- Our method only requires the sharing of an additional model-related gradient, without any information from the data or features themselves. Comprehensive comparative experiments and ablation results demonstrate the effectiveness of our method.

## 2 RELATED WORK

### 2.1 Federated Learning

Federated Learning is a paradigm for training models using decentralized client data while preserving privacy. Existing mature explorations have primarily focused on scenarios with heterogeneous client data, such as class imbalance in [18, 31, 43, 44]. Some efforts have concentrated on modifying local training in [19, 20, 25], with [20] adding L2 regularization between local and global models, [19, 25] performing contrastive learning locally. Other works [6, 34, 38] have rebuilt the aggregation strategy. All these approaches share a common goal, which is to tackle the challenge of training drift among clients caused by data heterogeneity. It's essential to note that this problem differs from domain generalization. The distribution of the test set in the former case remains a subset of that in the training set, which indicates it is already encountered by the model. In contrast, domain generalization extends to the test set from unseen domains (e.g., weather, scenes), where the distributions are unknown. While Yuan *et al.* [46] emphasized the importance of both types of research, our primary focus lies on domain generalization perspective. Because in the realm of multimedia, domain generalization presents a critical challenge owing to the high diversity and complexity of multimedia data. In open-world scenarios, the global model frequently encounters previously unseen data domains due to various factors such as collection environments, equipment disparities, and processing methodologies. Consequently, the model must possess robust generalization capabilities to accurately predict outcomes in the presence of these unfamiliar domains.

### 2.2 Domain Generalization

Domain generalization aims to enable models to make accurate predictions on domains that were not seen during training. Approaches in [17, 21, 26, 30, 32, 39] minimized domain gaps or learned domain-invariant features to achieve domain generalization. Meta-learning methods in [3, 7, 15] enhanced generalization capabilities by training models to "learn how to learn", but they were not programming-friendly. However, most of the above centralized methods require domain labels or direct access to multi-source domain data, which is constrained in the context of federated learning.

## 2.3 Federated Domain Generalization

Federated learning domain generalization is an emerging challenge that requires the global model to perform well on an unseen domain. Liu *et al.* [22] addressed it by sharing amplitude spectra-rich domain-related information, which is data-related and may lead to privacy leakage. Xu *et al.* [40] created a novel model selector to determine the closest model/data distribution for any test data. Zhang *et al.* [50] focused on aggregation, and improved the global model's generalization by reducing generalization differences between global and local models and increasing flatness in each domain. These methods still consider all features for prediction unbiasedly, which may lead the model to establish spurious short-cut correlations between data features and predictions. Consequently, when the model encounters unseen domain data, it may make incorrect predictions due to these confounders, even though the nature of the target remains unchanged. Therefore, we propose to intervene at the feature level during the federated training process by self-supervisedly training feature interveners to mitigate the adverse effects caused by spurious components. In the aggregation process, we further optimize the global model's cross-domain invariant prediction ability based on the theory of causal invariance.

## 3 PROPOSED METHOD

### 3.1 Problem Setting

**Motivation.** The generalization ability of *FL* is crucial for addressing open-world multimedia problems and advancing general artificial intelligence. Invariant Risk Minimization (*IRM*) theory suggests in [2] that models often capture spurious correlations in data, thereby impairing their ability to generalize. In the context of structural causal models, this issue arises from spurious correlations induced by data selection bias, where the true influences should come from causal invariant features.

The settings of *FL* have pros and cons for addressing this issue. Firstly, its diverse client-side heterogeneous data distributions can provide the global model with insights into a wider range of domains. However, its privacy-preserving nature means that these domain features related to the data are not easily shared like in a centralized manner.

Additionally, many centralized methods for removing spurious correlations are based on **strong prior knowledge** and have **constraints**. For example, methods that remove style information confounder [11] and background information confounder [29, 36] are based on the strong prior assumption that these types of information should not be causally related to the prediction. However, their constraints lie in the fact that their specificity to the objectives based on the above priors, thus can only remove the influence of one type of spurious correlated features at a time. It was also pointed out in [41] that the inadequacy of prior-based methods and found that causal features  $s_{cau}$  should actually be included in domain-invariant ones  $s_{com}$ , while domain-private features  $s_{pri}$ , which is variant, are contained in non-causal ones  $s_{non}$ , so there is:

$$\begin{cases} s_{cau} \subset s_{com}, \\ s_{non} \supset s_{pri}. \end{cases}$$

Therefore, when seeking to address the federated domain generalization problem by tackling spurious correlations, we need to avoid strong prior dependence on causal invariant components of images and the resulting constraints as much as possible. Thus, we directly apply the theory of invariance on the feature space to obtain a more general approach.

**Formulation.** In the federated learning framework, we consider that each client's data corresponds to a specific environment  $\epsilon$ . All clients together form the training environment set for federated learning, denoted as  $\mathcal{E}_{tr} = \{\epsilon_1, \dots, \epsilon_e, \dots, \epsilon_E\}$ , where  $E$  corresponds to the total number of clients. The data distribution of the  $e$ -th client is represented by  $P(\mathcal{X}_e, \mathcal{Y}_e | \epsilon_e)$ , where  $\mathcal{X}_e$  and  $\mathcal{Y}_e$  respectively denote the raw data and labels of client  $e$  with environment  $\epsilon_e$ . Each client conducts local training with the objective of  $\arg \min_{\theta} \mathcal{L}_e(\mathcal{X}_e, \theta_e^r)$  in communication round  $r$  ( $1 \leq r \leq R$ ). Subsequently, clients upload their local models  $\theta_e^r$  to the server, where aggregation  $\theta^r = \sum_{e=1}^E \frac{N_e}{N} \theta_e^r$  is performed to obtain the global model  $\theta^r$  in round  $r$ , where  $N_e$  denotes the number of samples on client  $e$  that participate in the training, and  $N$  denotes total number of samples involved in training across all clients. Therefore, the global objective of federated learning can be expressed as:

$$\arg \min_{\theta} \sum_{e=1}^E \frac{N_e}{N} \mathcal{L}_e(\mathcal{X}_e, \theta). \quad (1)$$

For domain generalization, Eq. 1 will undergo some changes. The global model needs to make accurate predictions in the environment  $\epsilon_{e'} \in \mathcal{E}' = \{\epsilon_{1'}, \dots, \epsilon_{e'}, \dots, \epsilon_{E'}\}$  of unseen domains. This requires the model to generalize well across diverse and previously unseen environments, with the goal of:

$$\arg \min_{\theta} \max_{\epsilon_{e'} \in \mathcal{E}'} \mathcal{L}(f(\mathcal{X}_{e'}; \theta), \mathcal{Y}_{e'} | \epsilon_{e'}). \quad (2)$$

Where  $f(\mathcal{X}_{e'}; \theta)$  represents the prediction obtained using the global model  $\theta$  on data  $\mathcal{X}_{e'}$ ,  $\mathcal{L}$  quantifies the error between this prediction and the true label  $\mathcal{Y}_{e'}$ .

### 3.2 Invariant Optimization Theory

We propose an efficient module, namely *SCI*, based on the principles of invariance to reduce spurious correlations at the client level, and provide a theoretical derivation for this purpose.

**Optimization objective.** It was suggested in [13] that causality-based out-of-distribution (*OOD*) studies, which include domain generalization issues, imply the existence of a feature subset  $F^S = \{F^s; s \in S\}$  such that the predictions generated using these features exhibit invariance across domains, i.e., they are independent of the environment  $\epsilon$ ,  $P(Y | F^S, \epsilon_i) = P(Y | F^S, \epsilon_{j \neq i}) = P(Y | F^S)$ .

In our approach, we aim to design interveners for features to reduce spurious correlations by weakening the feature components to varying degrees, that is,  $F^S := M_{\delta}(X)$ , where  $M_{\delta}(\cdot)$  is  $\delta$  parameterized and acts as a spurious feature intervener. So our optimization objective is to minimize the KL divergence:

$$d_{KL}[P(Y | M_{\delta_e}(X), \epsilon_e) || P(Y | M_{\delta_e}(X))], \forall \epsilon_e \in \mathcal{E}_{tr}, \quad (3)$$

and can be further written as:

$$\arg \min_{\delta_e} \mathbb{E}_{\mathcal{E}_{tr}} [d_{KL}(P(Y | M_{\delta_e}(X), \mathcal{E}_{tr}) || P(Y | M_{\delta_e}(X)))], \quad (4)$$

which is optimized through the learnable parameter  $\delta_e$  for every client with domain environment  $\epsilon_e \in \mathcal{E}_{tr}$ .

**Invariance-based simplification.** We still cannot obtain the relationship between the available intervener optimization objective and the learnable parameter  $\delta$  to generate it only through Eq. 4. Fortunately, [13] further manifests this connection in a centralized setting as shown in Eq. 5.

$$\begin{aligned} & \mathbb{E}_{\mathcal{E}_{tr}} [d_{KL}(P(Y|M_\delta(X), \mathcal{E}_{tr}) || P(Y|M_\delta(X)))], \\ &= \mathbb{E}_{\mathcal{E}_{tr}} [\log P(Y|M_\delta(X), \mathcal{E}_{tr}) - P(Y|M_\delta(X))], \\ &= \alpha (\mathbb{E}_{\mathcal{E}_{tr}} [\nabla_\delta \mathcal{L}_{\mathcal{E}_{tr}}(\delta)]^T \nabla_\delta \mathcal{L}_{\mathcal{E}_{tr}}(\delta)) \\ &\quad - \mathbb{E}_{\mathcal{E}_{tr}} [\nabla_\delta \mathcal{L}_{\mathcal{E}_{tr}}(\delta)]^T \mathbb{E}_{\mathcal{E}_{tr}} [\nabla_\delta \mathcal{L}_{\mathcal{E}_{tr}}(\delta)] + O(\alpha^2), \\ &= \alpha \text{trace}(\text{Var}_{\mathcal{E}_{tr}}(\nabla_\delta \mathcal{L}_{\mathcal{E}_{tr}}(\delta))) + O(\alpha^2), \end{aligned} \quad (5)$$

where  $\mathcal{L}_{\mathcal{E}_{tr}}(\delta) = \mathbb{E}_{(X,Y) \in \mathcal{E}_{tr}} [l(Q(Y|X; \delta), Y) | \mathcal{E}_{tr}]$  can be considered as the average predicted loss after using  $\delta$  to generate intervener for all data  $(X, Y) \in \mathcal{E}_{tr}$  of the whole training set,  $Q(\cdot)$  is the corresponding black-box system and only appears as an intermediate variable in the derivation.  $\alpha$  can be considered as the learning rate for  $\delta$ , and we have  $\delta' = \delta - \alpha \nabla_\delta \mathcal{L}_{\mathcal{E}_{tr}}(\delta)$ . It is important to note that our setup differs from the centralized methods described above in two key aspects:

1. In the centralized setup, the environment set  $\mathcal{E}_{tr}$  is considered as a whole. However, in the federated setting, each  $\epsilon_e$  corresponds to an individual client  $e$ . Therefore, we need to emphasize again that  $\epsilon_e \in \mathcal{E}_{tr} = \{\epsilon_1, \dots, \epsilon_e, \dots, \epsilon_E\}$ , meaning that we approach this problem from a client-wise perspective.

2. The centralized method described above can train a single  $\delta$  without distinguishing the heterogeneity of each  $\epsilon_e \in \mathcal{E}_{tr}$ , as they are considered as a whole. However, this is not applicable to our setup as described in aspect 1, because  $\mathcal{E}_{tr}$  cannot be accessed directly and in its entirety by any media. Thus, we generate a personalized  $M_{\delta_e}(\cdot)$  with learnable parameter  $\delta_e$  for each client  $e$  using Eq 4. Additionally, all averaging operations  $\mathbb{E}_{\mathcal{E}_{tr}}$  are replaced with client-wise averaging  $\mathbb{E}_c$ . Therefore, the overall train-set average loss is modified to be intra-client, as shown in Eq. 6.

$$\mathcal{L}_{\epsilon_e}(\delta_e) = \mathbb{E}_{(X_e, Y_e) \in \epsilon_e} [l(Q(Y_e|X_e; \delta_e), Y_e) | \epsilon_e], \quad \epsilon_e \in \mathcal{E}_{tr}. \quad (6)$$

For simplicity, the gradient of the  $\mathcal{L}_{\epsilon_e}(\delta_e)$  is denoted as:

$$\nabla_{\delta_e} \mathcal{L}_{\epsilon_e}(\delta_e) := \nabla_e, \quad e \in [1, \dots, e, \dots, E], \quad (7)$$

and each  $\nabla_e$  is considered separately.

Therefore, we take the intermediate term from Eq. 5 to create a new optimization objective:

$$\begin{aligned} & \min \underbrace{\mathbb{E}_c [\nabla_{\delta_e} \mathcal{L}_{\epsilon_e}(\delta_e)]^T \nabla_{\delta_e} \mathcal{L}_{\epsilon_e}(\delta_e)}_{\text{term 1}}, \\ & \quad - \underbrace{\mathbb{E}_c [\nabla_{\delta_e} \mathcal{L}_{\epsilon_e}(\delta_e)]^T \mathbb{E}_c [\nabla_{\delta_e} \mathcal{L}_{\epsilon_e}(\delta_e)]}_{\text{term 2}}, \end{aligned} \quad (8)$$

and derive these two terms separately. For the first term, we can

## Predict on an unseen domain

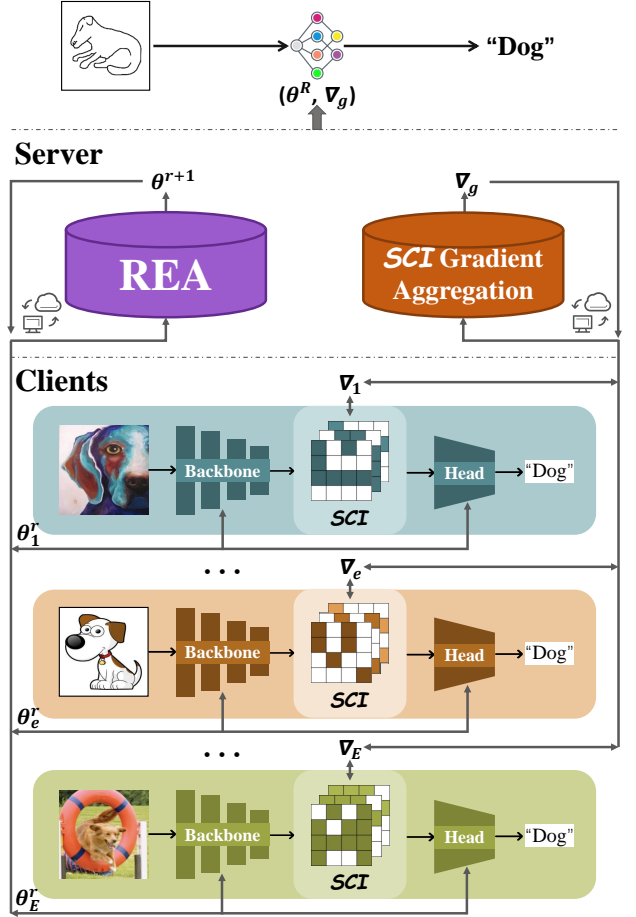


**Figure 2: A brief overview of FedCD, consisting of two components SCI and REA. In SCI, each client  $e$  compute a gradient alignment penalty using Eq. 14 and upload the local SCI gradient tensors  $\nabla_e$  in each communication round. They are then aggregated on the server to obtain  $\nabla_g$ , which is returned to the clients for the next round. REA determines aggregation coefficients through mathematical optimization based on Empirical Risk Minimization (ERM). Instead of introducing new neural network solutions for optimization, REA employs sequential least squares.**

intuitively obtain:

$$\begin{aligned} & \mathbb{E}_c [\nabla_{\delta_e} \mathcal{L}_{\epsilon_e}(\delta_e)]^T \nabla_{\delta_e} \mathcal{L}_{\epsilon_e}(\delta_e), \\ &= \mathbb{E}_c [\nabla_e^T \nabla_e], \\ &= \sum_{e=1}^E p_e \nabla_e^2, \end{aligned} \quad (9)$$

here we adopt the simplified form of 7, and concisely write  $\nabla_e^T \nabla_e$  as  $\nabla_e^2$ .  $p_e$  represents the probability of each client, serving as the aggregation coefficient of FedAvg, i.e.,  $p_e = \frac{N_e}{N}$ .

For the second term, we have:

$$\begin{aligned}
& \mathbb{E}_c[\nabla_{\delta_e} \mathcal{L}_{e_e}(\delta_e)]^T \mathbb{E}_c[\nabla_{\delta_e} \mathcal{L}_{e_e}(\delta_e)], \\
& = \mathbb{E}_c[|\nabla_e| \mathbf{1}_{1 \leq e \leq E}]^T \mathbb{E}_c[|\nabla_e| \mathbf{1}_{1 \leq e \leq E}], \\
& = \left( \sum_{e=1}^E p_e \nabla_e \right)^T \left( \sum_{e=1}^E p_e \nabla_e \right), \\
& = \nabla_g^2.
\end{aligned} \tag{10}$$

It can be observed that the penultimate term in Eq. 10 bears similarities to federated aggregation. Thus we define the global *SCI* gradient  $\nabla_g$  as  $\nabla_g := \sum_{e=1}^E p_e \nabla_e$ .

Therefore, the global objective of *SCI* is updated to Eq. 11,

$$\min \left| \sum_{e=1}^E p_e \nabla_e^2 - \nabla_g^2 \right|. \tag{11}$$

The absolute value is taken here because the original objective using  $d_{KL}$  is always greater than zero.

Since  $p_e$  is a fixed constant, we can consider that each client has the optimization objective:

$$\min |\nabla_e^2 - \nabla_g^2|. \tag{12}$$

This requires two tensor multiplication operations. To streamline computations, we aim to reduce it to a single tensor multiplication by analyzing the specific form of  $\nabla_g$ , and there is:

$$\begin{aligned}
& |\nabla_e^2 - \nabla_g^2| = |\nabla_e - \nabla_g| \cdot |\nabla_e + \nabla_g|, \\
& = |\nabla_e - \nabla_g| \cdot \left| \sum_{i=1, i \neq e}^E p_e \nabla_e + (1 + p_e) \nabla_e \right|, \\
& = |\nabla_e - \nabla_g| \cdot \left| \sum_{i=1, i \neq e}^E p_e \nabla_e + \beta \nabla_e \right|, \\
& \rightarrow |\nabla_e - \nabla_g| \cdot \left| \sum_{i=1, i \neq e}^E p_e \nabla_e + (p_e - 1) \nabla_e \right|_{\beta=(p_e-1)}, \\
& = |\nabla_e - \nabla_g| \cdot \left| \nabla_e - \sum_{i=1}^E p_e \nabla_e \right|, \\
& = |\nabla_e - \nabla_g|^2.
\end{aligned} \tag{13}$$

Because  $(1 + p_e)$  is a constant, we can treat it as a coefficient  $\beta$ . Then, we set  $\beta = (p_e - 1)$  and derive the final form based on the properties of absolute value. We continue to use the simplified notation  $|\nabla_e - \nabla_g|^2 := |\nabla_e - \nabla_g|^T |\nabla_e - \nabla_g|$  here.

Finally, the local training loss for *SCI* is in the form of the L2 norm, requiring only one tensor multiplication:

$$L_{SCI} = \|\nabla_e - \nabla_g\|^2. \tag{14}$$

Note that here  $\nabla_e$  represents the gradient of the loss function with respect to  $M_{\delta_e}(\cdot)$ , which is the gradient generated by the optimizer for learning the parameters  $\delta_e$ , and is different from that of the model parameters in the neural network.

In practical applications,  $M_{\delta_e}(\cdot)$  can take on various forms. Here, for computational efficiency, we consider a straightforward approach of feature masking, defining  $M_{\delta_e}(X) := M_e \odot X$ , where  $\odot$  represents element-wise multiplication. Additionally, previous

methods based on sharing often require each client to upload multiple components related to the data, forming a bank on the server for exchange, such as amplitude spectra [22, 23], image features [4], leading to communication and memory costs. In our approach, regardless of the data distribution, each client only needs to share a single gradient information, making it more lightweight.

### 3.3 SCI Implement

For each client  $e$ , the final training loss is:

$$L_e = L + \lambda L_{SCI}, \tag{15}$$

where  $\lambda$  is a hyperparameter and  $L$  depends on the form of downstream tasks, such as classification loss or object detection loss. As shown in Figure 2, each client  $e$  has one or more intervener optimizers for generating invariant masks. In each communication round, clients upload the *SCI* gradients  $\nabla_e$ , which are aggregated on the server using the *FedAvg* strategy to obtain  $\nabla_g$ , which is then distributed to all clients for the next round of computation.

Additionally,  $M_{\delta_e}(\cdot)$  is self-supervised generated, and there is no need for prior knowledge about causal invariance information. So it is not specifically designed for a particular type of confounder, but rather for the entire feature space, and thus can remove more types of confounders, i.e., spurious correlations.

### 3.4 REA Strategy

In the aforementioned efforts, we primarily focused on tasks conducted locally on the clients to enhance the domain generalization performance. Next, aiming to improve the global model's causal-invariant predictions, we introduce a novel aggregation strategy *REA* that determines the aggregation coefficients for the global model through solving an optimization problem related to risk extrapolation, which does not require new neural networks on the server, and is instead solved through sequential least squares.

The standard approach to solve the issue through risk extrapolation is *Empirical Risk Minimization (ERM)*. *ERM* involves minimizing the average training risks across all domains as shown in Eq. 16, where  $\ell$  is the loss function, often assumed to be fixed across different domains, and  $\theta$  denotes the model parameters of the neural network.  $\mathcal{R}_{e_q}(\theta)$  represents the risk of environment  $e_q$ , and  $Deq(x, y)$  represents the corresponding data,

$$\mathcal{R}_{ERM}(\theta) = \sum_{q=1}^Q |Deq| \mathbb{E}_{(x,y) \sim Deq} \ell(f_{\theta}(x), y). \tag{16}$$

In summary, this approach has two objectives:

1. Reduce training risk.
2. Enhance the similarity of training risks among domains.

Within the framework of federated learning, the first objective can be achieved through local learning. During the aggregation process, our focus is primarily on the second point. Krueger *et al.* [14] suggested that optimizing the model using cross-domain risk variance can lead to a flatter "risk plane". Additionally, it provides a smoother gradient vector field during training, meaning the vectors of its loss function can curve more smoothly toward the origin. Compared to other methods such as *Invariant Risk Minimization (IRM)* in [2], this smoother optimization landscape offers robust improvements. Therefore, we design a novel aggregation strategy.

Following the same symbol definitions,  $\mathcal{R}_e(\theta_e^r)$  denotes the training risk of each client, where we use  $L_e$  in Eq. 15. Assuming aggregation coefficients  $w = \{w_1, \dots, w_E\}$ , we can straightforwardly consider the client risks mapped globally as  $\mathcal{R}_{g_e}(\theta_e^r) = w_e \mathcal{R}_e(\theta_e^r)$ , similarly to how the global loss is considered in Eq. 1.

Hence, the aggregation coefficients correspond to the solution of the following risk extrapolation optimization problem as:

$$\min_w \text{Var}(\mathcal{R}_{g_1}(\theta_1^r), \mathcal{R}_{g_2}(\theta_2^r), \dots, \mathcal{R}_{g_E}(\theta_E^r)), \quad (17)$$

$$\text{s.t. } \mathcal{R}_{g_e}(\theta_e^r) = w_e \mathcal{R}_e(\theta_e^r), \quad (17a)$$

$$\sum_{e=1}^E w_e = 1, \quad (17b)$$

$$w_e > 0, \quad (17c)$$

$$1 \leq e \leq E. \quad (17d)$$

To account for the impact of sample sizes on the global model and combine  $w$  with the aggregation coefficients  $p_e$  of *FedAvg*, we normalize them to obtain the final aggregation coefficients  $C = \{c_1, \dots, c_e, \dots, c_E\}$  as follows:

$$c_e = \frac{\exp(\eta w_e + p_e)}{\sum_{k=1}^K \exp(\eta w_k + p_k)}, \quad (18)$$

where  $\eta$  is hyperparameter, denoting the contribution of *ERM*.

## 4 EXPERIMENTS

### 4.1 Experimental Setup

**Datasets.** We conducted simulations on both classification tasks with *ResNet18* [8] network and object detection tasks with *YOLOv5* network using different setups. For the classification tasks, we mainly simulated style generalization on the *PACS* [16] dataset. As for the object detection tasks, we used three autonomous driving datasets, namely *BDD100K* [45], *Cityscapes* [5], and *Mapillary* [1], to simulate dataset generalization, which exhibits larger domain shifts compared to other configurations. We also simulated scene generalization, especially on the *BDD100K* dataset.

**Implemented details.** Our proposed method is implemented in PyTorch, and experiments are conducted with different values for  $\lambda = \{0.5, 0.7, 0.8, 0.9, 1.0\}$ , and  $\eta = \{0.3, 0.5, 0.8\}$ , with results provided for the optimal parameter configurations.

Each mask  $M_{\delta_e}(\cdot)$  is initialized to an all-1 tensor, or all-pass, to avoid removing too many features at the beginning of training, which could prevent the model from learning correctly.

For the object detection task, we run the experiments on a workstation with NVIDIA A100 GPUs. We set the batch size to 4, conduct a total of 200 communication rounds, and perform 1 local training epoch in each round. The learning rate is set to  $1.6 \times 10^{-4}$ .

For the classification task, we run the experiments on NVIDIA GeForce RTX 4060 GPUs, with a batch size of 16. We conduct a total of 40 communication rounds, and each round consists of 5 epochs of local training. The learning rate is set to 0.001.

**Table 1: Style generalization. Training results for accuracy *Acc*(%) and average accuracy *AA*(%) on four styles in the *PACS* dataset, which are Photo (P), Art painting (A), Cartoon (C) and Sketch (S). The table header represents the current testing style, following the ‘leave-one-domain-out’ principle, where each of the three clients corresponds to one of the remaining three styles (domains).**

| Algorithm                      | P            | A            | C            | S            | AA           |
|--------------------------------|--------------|--------------|--------------|--------------|--------------|
| ARFL [35]                      | 92.10        | 76.25        | 75.79        | 80.47        | 81.15        |
| FedAvg [24]                    | 92.77        | 77.29        | 77.97        | 81.03        | 82.27        |
| FedDG-GA [50]                  | 93.97        | 81.28        | 76.73        | 82.57        | 83.64        |
| FedCSA [6]                     | 91.88        | 77.00        | 76.79        | 80.84        | 81.63        |
| FedNova [38]                   | 94.03        | 79.93        | 76.39        | 79.26        | 82.40        |
| FedProx [20]                   | 93.15        | 77.72        | 77.73        | 80.77        | 82.34        |
| FedSAM [28]                    | 91.20        | 74.45        | 77.77        | 83.35        | 81.69        |
| FedADG [47]                    | 92.93        | 77.85        | 74.74        | 79.54        | 81.27        |
| HarmoFL [10]                   | 90.99        | 74.51        | 77.43        | 81.73        | 81.17        |
| Scaffold [12]                  | 92.50        | 78.09        | 77.23        | 80.67        | 82.12        |
| FedSR [27]                     | 93.82        | <b>83.24</b> | 76.03        | 82.11        | 83.80        |
| FedCMI                         | 92.85        | 80.84        | 73.72        | 79.52        | 81.73        |
| FedL2R                         | 92.84        | 82.24        | 75.83        | 81.61        | 83.13        |
| AM                             | 93.29        | 80.86        | 77.62        | 81.05        | 83.21        |
| RSC [9]                        | 92.67        | 77.98        | 77.80        | 82.90        | 82.84        |
| SNR [11]                       | <b>94.54</b> | 80.32        | 78.23        | 74.12        | 81.80        |
| FedCD- <i>SCI</i>              | 94.13        | 82.27        | 79.05        | 83.66        | 84.78        |
| FedCD- <i>SCI</i> + <i>REA</i> | 94.42        | 82.58        | <b>79.35</b> | <b>84.00</b> | <b>85.09</b> |

### 4.2 Experimental Results

**Style generalization.** Table 1 shows the contribution of *FedCD* to style generalization. It can be observed that our method achieves an average *Acc* increase of at least 1.45% over the baselines when using both *SCI* and *REA*, and at least 1.14% when using only *SCI*. *AM*, i.e., Amplitude Mix, is a powerful Fourier-based augmentation method widely used in many *DG* methods [37, 42, 49]. Notably, our method achieves a slightly lower *Acc* of 0.12% compared to *SNR* when the test style is ‘‘P’’, which is a centralized method specifically designed to remove style confounder. However, our average *Acc* surpasses it by 3.29%, with a more stable performance, as indicated by a variance that is 0.54× smaller than that of *SNR*.

*FedSR* is a federated learning algorithm that enhances the generalization performance of federated learning through representation and conditional mutual information regularization. It can be seen that its *Acc* is 0.66% higher than our method when the test domain is ‘‘S’’, but its average *Acc* is 1.29% lower than ours. Our method is also more robust than it, with a variance in *Acc* that is 0.78× smaller.

**Dataset/Scene generalization.** In the dataset generalization setting shown in Table 2, *FedCD* achieves an average *mAP*<sub>50</sub> increase of at least 4.8% over baselines when using both *SCI* and *REA*, and at least 3.14% when using only *SCI*. In the scene generalization setting shown in Table 3, *FedCD* achieves an average *mAP*<sub>50</sub> increase of at least 1.27% over baselines when using both *SCI* and



**Table 2: Dataset generalization. Training results for  $mAP_{50}$  (%) and average  $mAP_{50}$  Avg(%) in three datasets (domains) in Cityscapes (C), Mapillary (M) and BDD100K (B), with "leave-one-domain-out".**

| Algorithm       | C            | M            | B            | Avg          |
|-----------------|--------------|--------------|--------------|--------------|
| FedAvg          | 43.39        | 35.49        | 39.69        | 39.52        |
| FedProx         | 44.10        | 35.56        | 40.10        | 39.92        |
| FedSAM          | 43.61        | 33.77        | 44.14        | 40.51        |
| FedDG-GA        | 43.75        | 35.49        | 40.94        | 40.06        |
| FedCD-SCI       | 46.47        | 40.00        | 44.50        | 43.65        |
| FedCD-SCI + REA | <b>46.67</b> | <b>41.37</b> | <b>46.56</b> | <b>44.86</b> |

**Table 3: Scene generalization. Training results for  $mAP_{50}$  (%) and average  $mAP_{50}$  Avg(%) in four scenes (domains), ClearHighway (CH), RainyHighway (RH), CityStreet (CS), Residential (RE), within BDD100K dataset, with the "leave-one-domain-out" principle.**

| Algorithm       | CH           | RH           | CS           | RE           | Avg          |
|-----------------|--------------|--------------|--------------|--------------|--------------|
| FedAvg          | 37.98        | 38.26        | 41.91        | 45.21        | 40.84        |
| FedProx         | 38.69        | 38.89        | 41.82        | 44.46        | 40.97        |
| FedSAM          | 38.44        | 39.77        | 40.31        | 46.04        | 41.14        |
| FedDG-GA        | 39.05        | 39.74        | 41.86        | 45.91        | 41.64        |
| FedCD-SCI       | 41.44        | 38.81        | 41.21        | 46.58        | 42.26        |
| FedCD-SCI + REA | <b>41.69</b> | <b>39.78</b> | <b>43.11</b> | <b>47.05</b> | <b>42.91</b> |

REA, and at least 0.62% when using only SCI. Both of these scenarios demonstrate very small variances of 6.12(%<sup>2</sup>) and 7.12(%<sup>2</sup>), respectively, indicating the stability of our method's performance.

It is worth noting that our approach yields greater performance improvements in the dataset generalization setting with larger domain shifts. We attribute this to the inherent generalization capability of neural networks, which can to some extent address stable predictions with smaller domain shifts. Therefore, the improvement brought by our approach appears relatively small.

### 4.3 Analyses on SCI

**Sparsity analysis.** We continuously observed the  $L1$  norm of the average mask on randomly sampled batches during training. For more details, we conducted experiments under each "leave-one-domain-out" setting with  $\lambda = \{0.7, 0.9\}$  respectively, and the results are shown in Figure 3. We calculated the  $L1$  norm of all masks generated on each participating client. Subsequently, we averaged these norms both within each client and across all clients. This process allowed us to observe the trend of the  $L1$  norm with the total training epochs of federated learning.

We can observe from Figure 3 that, the  $L1$  norm of the mask shows a decreasing trend for different settings of  $\lambda$  and leave-out domain. Since the  $L1$  norm is essentially a sparse operator, this indicates that features tend to become sparse during the federated training. This is actually consistent with the insight provided by

$FedL2R$  in [27], which directly utilizes the regularization term:

$$l^{L2R} = \mathbb{E}_{p_i(z)} [\|z\|_2^2], \quad (19)$$

where  $z$  represents the intermediate feature representation of the network. Using the same notation, we can consider  $z = M_{\delta_e}(x) = M_e \odot x$ , where for a sparser  $M_e$ , a sparser  $z$  can be generated, resulting in a smaller  $l^{L2R}$ .

Assuming there exists a "reference" distribution  $q(z) = \mathcal{N}(0, \sigma^2 I)$  (with a small  $\sigma$ ), we have:

$$-\log q(z) = \frac{\|z\|_2^2}{2\sigma^2} + C, \quad (20)$$

where  $C$  is an additive constant.

We can consider incorporating  $q(z)$  into the calculation of  $l^{L2R}$ :  $l^{L2R} = \mathbb{E}_{p_i(z)} [\|z\|_2^2] = 2\sigma^2 \mathbb{E}_{p_i(z)} [-\log q(z)] = 2\sigma^2 H(p_i(z), q(z))$ , (21)

where  $H(p_i(z), q(z))$  denotes the cross entropy from  $p_i(z)$  to the reference distribution  $q(z)$ .

The Eq. 21 can be rewritten in the form of KL divergence:

$$H(p_i(z), q(z)) = H(p_i(z)) + KL[p_i(z)||q(z)]. \quad (22)$$

Therefore, if the entropy  $H(p_i(z))$  remains relatively stable dur-

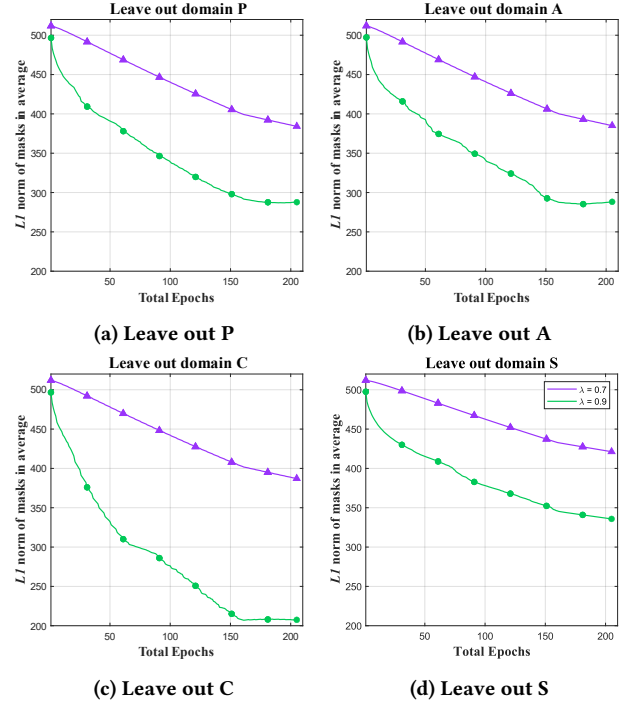


**Figure 3: Comparing the average  $L1$  norm of the masks generated by SCI under different hyperparameters  $\lambda = 0.7/0.9$  and different "leave-one-domain-out" settings.**

ing training, minimizing  $l^{L2R}$  will also minimize  $KL[p_i(z)||q(z)]$ , which encourages  $p_i(z)$  to be close to  $q(z)$ , implying an implicit alignment of the marginal distribution. Therefore, our method also aligns the feature distributions of each client to some extent, establishing a connection with domain-invariant representation learning,

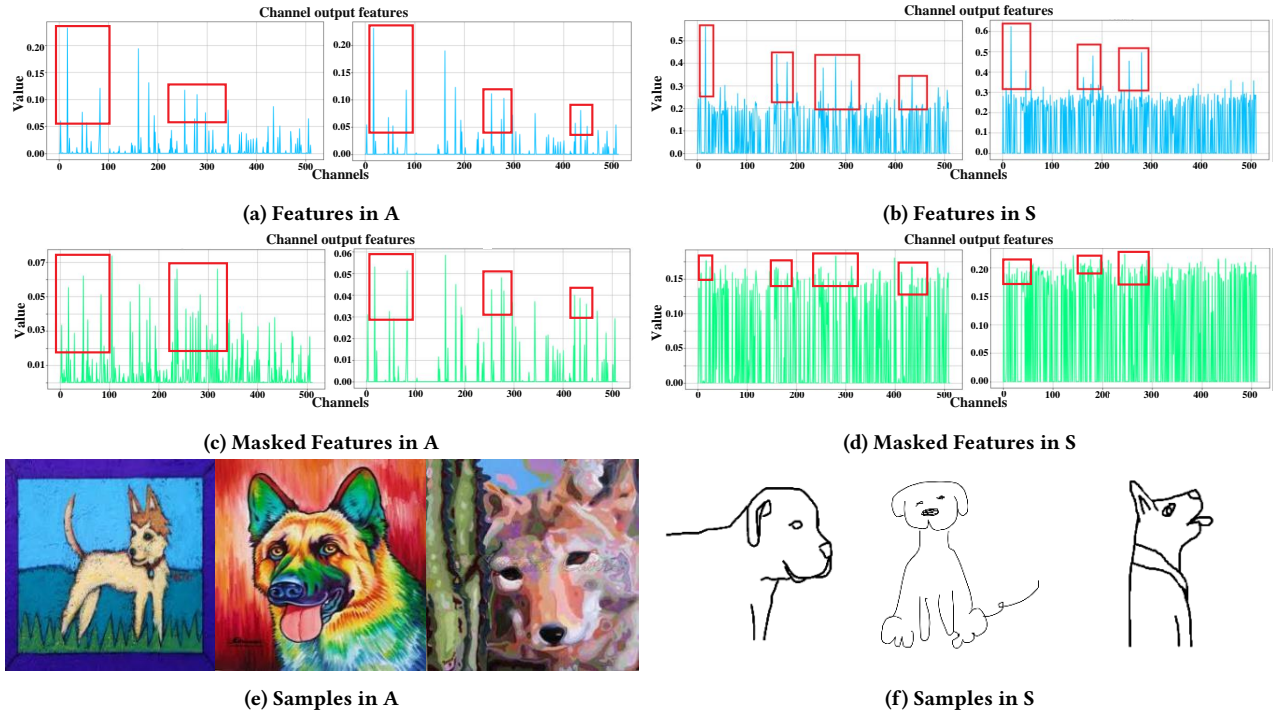


**Figure 4: The comparison between the original features and masked features of samples from feature-rich domain Art painting (A) and feature-poor domain Sketch (S), which reflects two phenomena: a decrease in overall and a decrease in specificity.**

thereby improving generalization. However, our method achieves an *Acc* 1.65 higher than *FedL2R* when using only *SCI*, which reflects the gain from considering the additional spurious correlations.

#### 4.4 DISCUSSION

**Masked feature analysis.** Next, we analyzed the feature outputs before and after adding the mask. In the experiment setting of leaving out "P", we took the *art painting* style with rich features and the *sketch* style with fewer features as examples, as shown in Figure 4. Because we added a mask to the output of the *Avg\_pool* layer of *ResNet18*, which is channel-wise average pooling, we obtained a one-dimensional tensor, and our mask equivalently acts on all the feature pixels before pooling.

For both styles with rich features and styles with singular features, our masks exhibit two trends: a decrease in overall and a decrease in specificity.

The decrease in overall may correspond to some intra-channel overall spurious correlated features, such as background information, style information, etc., which exist in the feature maps of each channel. This actually corresponds to the conclusion in Section 4.3. As shown in Figure 4, the majority of original image feature values are 0.05 and 0.2 in domain "A" and "S". After adding masks, they are reduced to 0.03 and 0.15 respectively, with reduction factors of 1.7 $\times$  and 1.3 $\times$ . This indicates that for images like the ones in Figure 4e in domain "A", which may have more overall spurious shortcut information in each channel based on their own feature richness, we would produce an unbiasedly larger weakening compared to

samples that already have insufficiently rich information, like the ones in Figure 4f in domain "S".

Regarding the decrease in specificity, for the feature values highlighted by the red boxes in Figure 4a and Figure 4b, our mask can generate specific weakening, i.e., changes in relative size. This corresponds to the extraction of more spurious correlated features in certain channels. Furthermore, it can be observed that the masked feature in Figure 4d has a more uniform channel-wise distribution compared to Figure 4c. We believe this is because the features of domain "S" samples are singular, leading to more similar causally invariant features in each channel and thus forming a more uniform feature distribution.

#### 5 CONCLUSION

We primarily address the domain generalization issue in multimedia federated learning and propose a simple yet effective framework, *FedCD*, that reconsiders this problem from both local and global perspectives. In local level, our *SCI* differs from previous approaches, which considered all features unbiasedly during training. Instead, we generate feature interveners in a self-supervised manner based on the principle of invariance. This approach helps intervene and reduce the adverse effects of spurious shortcut features, all without requiring data or feature-related information sharing. Additionally, it does not rely on any prior knowledge of causal invariance components in the images, further expanding the scope of removing spurious features due to its nonspecific purpose. We provide theoretical derivations for our approach. On the server side, we introduce a novel aggregation module, *REA*, which utilizes *ERM*



to achieve better global causal invariant predictions by converting the aggregation coefficients into the solution of a mathematical optimization problem. This process can be solved by simply using sequential least squares without introducing new neural networks. Additionally, we conduct thorough ablation experiments and analysis to validate the effectiveness of our method in various tasks and generalization scenarios, demonstrating its robustness and scalability in complex multimedia datasets.

## REFERENCES

- [1] Manuel López Antequera, Pau Gargallo, Markus Hofinger, Samuel Rota Buló, Yubin Kuang, and Peter Kotschieder. 2020. Mapillary planet-scale depth dataset. In *the European Conference on Computer Vision*. Springer, 589–604.
- [2] Martin Arjovsky, Léon Bottou, Ishaan Gulrajani, and David Lopez-Paz. 2019. Invariant risk minimization. *arXiv preprint arXiv:1907.02893* (2019).
- [3] Yogesh Balaji, Swami Sankaranarayanan, and Rama Chellappa. 2018. MetaReg: Towards Domain Generalization using Meta-Regularization. In *Advances in Neural Information Processing Systems*, Vol. 31.
- [4] Junming Chen, Meirui Jiang, Qi Dou, and Qifeng Chen. 2023. Federated Domain Generalization for Image Recognition via Cross-Client Style Transfer. In *the IEEE/CVF Winter Conference on Applications of Computer Vision*. 361–370.
- [5] Marius Cordts, Mohamed Omran, Sebastian Ramos, Timo Rehfeld, Markus Endzweiler, Rodrigo Benenson, Uwe Franke, Stefan Roth, and Bernt Schiele. 2016. The cityscapes dataset for semantic urban scene understanding. In *the IEEE/CVF International Conference on Computer Vision*. 3213–3223.
- [6] Xinyu Dong, Zhenwei Shi, XiaoMei Huang, Chu Han, Zihan Cao, Zhihe Zhao, Dan Wang, Peng Xu, Zaiyi Liu, and Wenbin Liu. 2023. Fed-CSA: Channel Spatial Attention and Adaptive Weights Aggregation-Based Federated Learning for Breast Tumor Segmentation on MRI. In *International Conference on Intelligent Computing*. Springer, 312–323.
- [7] Qi Dou, Daniel Coelho de Castro, Konstantinos Kamnitsas, and Ben Glocker. 2019. Domain Generalization via Model-Agnostic Learning of Semantic Features. In *Advances in Neural Information Processing Systems*, Vol. 32.
- [8] Kaiming He, Xiangyu Zhang, Shaoqing Ren, and Jian Sun. 2016. Deep Residual Learning for Image Recognition. In *the IEEE/CVF International Conference on Computer Vision*.
- [9] Zeyi Huang, Haohan Wang, Eric P Xing, and Dong Huang. 2020. Self-challenging improves cross-domain generalization. In *the European Conference on Computer Vision*. Springer, 124–140.
- [10] Meirui Jiang, Zirui Wang, and Qi Dou. 2022. Harmofl: Harmonizing local and global drifts in federated learning on heterogeneous medical images. In *the AAAI Conference on Artificial Intelligence*, Vol. 36. 1087–1095.
- [11] Xin Jin, Cuiling Lan, Wenjun Zeng, and Zhibo Chen. 2021. Style normalization and restitution for domain generalization and adaptation. *IEEE Transactions on Multimedia* 24 (2021), 3636–3651.
- [12] Sai Praneeth Karimireddy, Satyen Kale, Mehryar Mohri, Sashank Reddi, Sebastian Stich, and Ananda Theertha Suresh. 2020. Scaffold: Stochastic controlled averaging for federated learning. In *International Conference on Machine Learning*. PMLR, 5132–5143.
- [13] Masanori Koyama and Shoichiro Yamaguchi. 2021. When is invariance useful in an Out-of-Distribution Generalization problem? *arXiv:2008.01883*
- [14] David Krueger, Ethan Caballero, Joern-Henrik Jacobsen, Amy Zhang, Jonathan Binas, Dinghui Zhang, Remi Le Priol, and Aaron Courville. 2021. Out-of-distribution generalization via risk extrapolation (rex). In *International Conference on Machine Learning*. PMLR, 5815–5826.
- [15] Da Li, Yongxin Yang, Yi-Zhe Song, and Timothy Hospedales. 2018. Learning to generalize: Meta-learning for domain generalization. In *the AAAI Conference on Artificial Intelligence*, Vol. 32.
- [16] Da Li, Yongxin Yang, Yi-Zhe Song, and Timothy M Hospedales. 2017. Deeper, broader and artier domain generalization. In *the IEEE/CVF International Conference on Computer Vision*. 5542–5550.
- [17] Haoliang Li, Sinno Jialin Pan, Shiqi Wang, and Alex C Kot. 2018. Domain generalization with adversarial feature learning. In *the IEEE/CVF Conference on Computer Vision and Pattern Recognition*. 5400–5409.
- [18] Qinbin Li, Yiqun Diao, Quan Chen, and Bingsheng He. 2022. Federated learning on non-iiid data silos: An experimental study. In *International Conference on Data Engineering*. IEEE, 965–978.
- [19] Qinbin Li, Bingsheng He, and Dawn Song. 2021. Model-contrastive federated learning. In *the IEEE/CVF Conference on Computer Vision and Pattern Recognition*. 10713–10722.
- [20] Tian Li, Anit Kumar Sahu, Manzil Zaheer, Maziar Sanjabi, Ameet Talwalkar, and Virginia Smith. 2020. Federated optimization in heterogeneous networks. In *Machine Learning and Systems*, Vol. 2. 429–450.
- [21] Ya Li, Xinmei Tian, Mingming Gong, Yajing Liu, Tongliang Liu, Kun Zhang, and Dacheng Tao. 2018. Deep domain generalization via conditional invariant adversarial networks. In *the European Conference on Computer Vision*. 624–639.
- [22] Quande Liu, Cheng Chen, Jing Qin, Qi Dou, and Pheng-Ann Heng. 2021. FedDG: Federated domain generalization on medical image segmentation via episodic learning in continuous frequency space. In *the IEEE/CVF Conference on Computer Vision and Pattern Recognition*. 1013–1023.
- [23] Fangrui Lv, Jian Liang, Shuang Li, Bin Zang, Chi Harold Liu, Ziteng Wang, and Di Liu. 2022. Causality inspired representation learning for domain generalization. In *the IEEE/CVF Conference on Computer Vision and Pattern Recognition*. 8046–8056.
- [24] Brendan McMahan, Eider Moore, Daniel Ramage, Seth Hampson, and Blaise Aguera y Arcas. 2017. Communication-Efficient Learning of Deep Networks from Decentralized Data. In *Conference on Artificial Intelligence and Statistics*. PMLR, Ft. Lauderdale, FL, 1273–1282.
- [25] Kutong Mu, Yulong Shen, Ke Cheng, Xueli Geng, Jiaxuan Fu, Tao Zhang, and Zhiwei Zhang. 2023. Fedproc: Prototypical contrastive federated learning on non-iiid data. *Future Generation Computer Systems* 143 (2023), 93–104.
- [26] Krikamol Muandet, David Balduzzi, and Bernhard Schölkopf. 2013. Domain generalization via invariant feature representation. In *International Conference on Machine Learning*. PMLR, 10–18.
- [27] A. Tuan Nguyen, Philip Torr, and Ser Nam Lim. 2022. FedSR: A Simple and Effective Domain Generalization Method for Federated Learning. In *Advances in Neural Information Processing Systems*, S. Koyejo, S. Mohamed, A. Agarwal, D. Belgrave, K. Cho, and A. Oh (Eds.), Vol. 35. 38831–38843.
- [28] Zhe Qu, Xingyu Li, Rui Duan, Yao Liu, Bo Tang, and Zhuo Lu. 2022. Generalized federated learning via sharpness aware minimization. In *International Conference on Machine Learning*. PMLR, 18250–18280.
- [29] Feifei Shao, Yawei Luo, Li Zhang, Lu Ye, Siliang Tang, Yi Yang, and Jun Xiao. 2021. Improving weakly supervised object localization via causal intervention. In *the ACM International Conference on Multimedia*. 3321–3329.
- [30] Rui Shao, Xiangyuan Lan, Jiawei Li, and Pong C Yuen. 2019. Multi-adversarial discriminative deep domain generalization for face presentation attack detection. In *the IEEE/CVF Conference on Computer Vision and Pattern Recognition*. 10023–10031.
- [31] Zebang Shen, Juan Cervino, Hamed Hassani, and Alejandro Ribeiro. 2021. An agnostic approach to federated learning with class imbalance. In *International Conference on Learning Representations*.
- [32] Yuge Shi, Jeffrey Seely, Philip HS Torr, N Siddharth, Awni Hannun, Nicolas Usunier, and Gabriel Synnaeve. 2021. Gradient matching for domain generalization. *arXiv preprint arXiv:2104.09937* (2021).
- [33] Yuwei Sun, Ng Chong, and Hideya Ochiai. 2023. Feature Distribution Matching for Federated Domain Generalization. In *Asian Conference on Machine Learning*, Vol. 189. PMLR, 942–957.
- [34] Md Palash Uddin, Yong Xiang, Borui Cai, Xuequan Lu, John Yearwood, and Longxiang Gao. 2023. ARFL: Adaptive and Robust Federated Learning. *IEEE Transactions on Mobile Computing* (2023).
- [35] Md Palash Uddin, Yong Xiang, Borui Cai, Xuequan Lu, John Yearwood, and Longxiang Gao. 2024. ARFL: Adaptive and Robust Federated Learning. *IEEE Transactions on Mobile Computing* 23, 5 (2024), 5401–5417. <https://doi.org/10.1109/TMC.2023.3310248>
- [36] Dong Wang, Yuewei Wang, Chenyang Tao, Zhe Gan, Liqun Chen, Fanjie Kong, Ricardo Henao, and Lawrence Carin. 2021. Proactive Pseudo-Intervention: Causally Informed Contrastive Learning For Interpretable Vision Models. *arXiv:2012.03369* [cs.CV]
- [37] Jingye Wang, Ruoyi Du, Dongliang Chang, and Zhanyu Ma. 2022. Domain generalization via frequency-based feature disentanglement and interaction. *CoRR* (2022).
- [38] Jianyu Wang, Qinghua Liu, Hao Liang, Gauri Joshi, and H. Vincent Poor. 2020. Tackling the Objective Inconsistency Problem in Heterogeneous Federated Optimization. In *Advances in Neural Information Processing Systems*, Vol. 33. 7611–7623.
- [39] Shujun Wang, Lequan Yu, Caizi Li, Chi-Wing Fu, and Pheng-Ann Heng. 2020. Learning from extrinsic and intrinsic supervisions for domain generalization. In *the European Conference on Computer Vision*. Springer, 159–176.
- [40] An Xu, Wenqi Li, Pengfei Guo, Dong Yang, Holger R Roth, Ali Hatamizadeh, Can Zhao, Daguang Xu, Heng Huang, and Ziyue Xu. 2022. Closing the generalization gap of cross-silo federated medical image segmentation. In *the IEEE/CVF Conference on Computer Vision and Pattern Recognition*. 20866–20875.
- [41] Mingjun Xu, Lingyun Qin, Weijie Chen, Shiliang Pu, and Lei Zhang. 2023. Multi-view adversarial discriminator: Mine the non-causal factors for object detection in unseen domains. In *the IEEE/CVF Conference on Computer Vision and Pattern Recognition*. 8103–8112.
- [42] Qinwei Xu, Ruipeng Zhang, Ya Zhang, Yanfeng Wang, and Qi Tian. 2021. A fourier-based framework for domain generalization. In *the IEEE/CVF Conference on Computer Vision and Pattern Recognition*. 14383–14392.
- [43] Rui Ye, Zhenyang Ni, Chenxin Xu, Jianyu Wang, Siheng Chen, and Yonina C Eldar. 2023. FedFM: Anchor-based feature matching for data heterogeneity in federated learning. *IEEE Transactions on Signal Processing* (2023).

- [44] Jaehong Yoon, Wonyong Jeong, Giwoong Lee, Eunho Yang, and Sung Ju Hwang. 2021. Federated continual learning with weighted inter-client transfer. In *International Conference on Machine Learning*. PMLR, 12073–12086.
- [45] Fisher Yu, Haofeng Chen, Xin Wang, Wenqi Xian, Yingying Chen, Fangchen Liu, Vashisht Madhavan, and Trevor Darrell. 2020. Bdd100k: A diverse driving dataset for heterogeneous multitask learning. In *the IEEE/CVF International Conference on Computer Vision*. 2636–2645.
- [46] Honglin Yuan, Warren Morningstar, Lin Ning, and Karan Singhal. 2021. What do we mean by generalization in federated learning? *arXiv preprint arXiv:2110.14216* (2021).
- [47] Liling Zhang, Xinyu Lei, Yichun Shi, Hongyu Huang, and Chao Chen. 2023. Federated Learning for IoT Devices With Domain Generalization. *IEEE Internet of Things Journal* 10, 11 (2023), 9622–9633. <https://doi.org/10.1109/JIOT.2023.3234977>
- [48] Lin Zhang, Yong Luo, Yan Bai, Bo Du, and Ling-Yu Duan. 2021. Federated Learning for Non-IID Data via Unified Feature Learning and Optimization Objective Alignment. In *the IEEE/CVF International Conference on Computer Vision*. 4400–4408.
- [49] Ruipeng Zhang, Qinwei Xu, Chaoqin Huang, Ya Zhang, and Yanfeng Wang. 2022. Semi-supervised domain generalization for medical image analysis. In *International Symposium on Biomedical Imaging*. IEEE, 1–5.
- [50] Ruipeng Zhang, Qinwei Xu, Jiangchao Yao, Ya Zhang, Qi Tian, and Yanfeng Wang. 2023. Federated domain generalization with generalization adjustment. In *the IEEE/CVF Conference on Computer Vision and Pattern Recognition*. 3954–3963.